Experimental and Numerical Study of CO_2/CH_4 Separation Using SAPO-34/PES Hollow Fiber Membrane

Omrani, Hannaneh; Naser, Iraj+; Rafie Zadeh, Mahdi***

Chemical Engineering Department, South Tehran Branch, Islamic Azad University, Tehran, I. R. IRAN

ABSTRACT: *In this work, the defects in poletherysulfone (PES)/silicoaluminophosphate (SAPO)-34 zeolite mixed matrix membrane was prepared by dry-wet spinning technique for the separation of CO_2/CH_4 mixtures. In this regard, the synthesized PES/SAPO-34 Mixed Matrix Membranes (MMMs) were characterized via FESEM analyses. The Response Surface Methodology (RSM) was applied to find the relationships between several explanatory variables such as air gap distance, jet stretch ratio, and zeolite content, and CO_2 permeance as responses. The results were validated with the experimental data, which the model results were in good agreement with the available experimental data. The effects of feed temperature and feed pressure on permeation and CO_2/CH_4 selectivity of membranes were investigated. The MMMs showed better performance than the neat PES membrane. A two-dimensional countercurrent mathematical model for membrane separation has been incorporated with Aspen HYSYS to optimize and design the membrane system for CO_2 capture from natural gas. Permeation results manifested that the PES/SAPO-34 fabricated at optimum conditions has incredible worth from the perspective of industrial separations of CO_2 from the flue and natural gas.*

KEYWORDS: *Hollow fiber; Membrane; SAPO 34; Polyethersulfone; CO_2 Separation.*

INTRODUCTION

Carbon dioxide (CO_2) is the largest concern of global warming in the past five years [1-3]. CO_2 is in natural gas streams, flue gas from fossil fuel combustion, and a product of coal gasification. The presence of CO_2 and other acid gases reduce the calorific value and make the gas streams become acidic and corrosive, which decrease gas compression and transport. Pipeline specifications usually need CO_2 concentrations below 2% [2]. One major step to treat the various gas streams is to remove acid gas such as CO_2, H_2S, and SO_2 before it is compressed and delivered[6]. Highly concentrated CO_2 can be produced from such separation processes rather than direct release into atmosphere. By pumping and storing pure or highly concentrated CO_2 deep underground, sequestration may provide one feasible approach to treating greenhouse gas emissions [4]. Therefore, economic and effective techniques for CO_2 removal from CH_4 and capture at a wide range of CO_2 concentration levels and flow rates are highly desirable and have attracted great interest [5].

The low capital and operating cost of membrane for removal of impurities from natural gas streams is growing rapidly. Gas permeation characteristics of PES-SAPO-34-HMA were investigated by *Elif et al.*[6]. The results proved that the permeability of all the gases through

** To whom correspondence should be addressed.*
+ E-mail: i_naser@azad.ac.ir
1021-9986/2021/3/841-852 12/$/6.02

PES-SAPO-34-HMA membranes was significantly more than those through PES/HMA membranes. New MMMs based on polymerizable room-temperature ionic liquids and SAPO-34 as filler were studied [7]. It was shown that increasing of ionic liquids in the MMMs, increases the CO_2 permeability. The effect of the addition of SAPO-34 as filler on the gas permeation properties of other polymers such polysulfone [8] has been researched. Gas separation studies in the field of adding SAPO-34 particles into the polyurethane matrix have been not reported before. The effect of silica particles on the permeation properties of polyurethane membranes was investigated [9]. The obtained results indicated the reduction in permeability of CO_2, CH_4, O_2 and N_2 gases. But enhancement of CO_2/CH_4, $CO_2/N_2$and O_2/N_2 selectivity by increasing silica content was observed. Lots of review papers provide a better understanding of the incorporation of inorganic fillers in MMMs' and the outlook of fillers for CO_2/CH_4 and CO_2/N_2 separation [10].

In this research, the gas separation properties of PES-SAPO 34 hollow fiber MMMs were explored. The hollow fiber membranes were spun from polymer solution containing PES/modified SAPO 34 at various zeolite loading, air gap distance and dope extrusion rate. In order to verify the effect of these parameters on CO_2 and CH_4 permeance, response surface methodology (RSM) based on central composite design (CCD) was used. Recently, response surface method (RSM) is a mathematical and statistical method employed for modeling and optimization of numerous processes. Central Composite Design (CCD) in the RSM is a main design tool used for optimization of methods. The CCD provides complete results and detailed information even for a small number of experiments and positive effects of operating parameters on all responses. The effects of operational parameters such as pressure, temperature and gas composition on permeability (CO_2 and CH_4 gases) and selectivity of those membranes were further studied. The paper also demonstrates the numerical study of CO_2 removal from natural gas through adaptation of proposed hollow fiber membrane module to compare the performance of different flow configurations based on their separation efficiency and process economics. As membrane unit is not a pre-defined unit operation in Aspen Plus, membrane model is included in the process simulation as user defined unit operation along with other available unit operations using A FORTRAN sub-routine.

MATERIALS AND METHODS

MMMs were prepared using PES as polymer matrix due to its excellent thermal and mechanical characteristics. SAPO-34 is a proven facilitator for better CO2/CH_4 separation. CO_2 gas (99.99% purity) was purchased from Farafan Gas Co. (Isfahan, Iran) and CH_4 gas was acquired from Air Products Co. (Tehran, Iran). Other chemicals were taken from Sigma Alderich (USA).

Membrane preparation

SAPO-34 zeolite was synthesized via hydrothermal method [11]. Asymmetric porous SAPO-34/PES hollow fiber membranes were prepared by the dry–wet spinning technique according to the phase inversion process. Bore fluid was prepared by dissolving SAPO-34 nanoparticles in solvent followed by gentle stirring for 24 h until a homogenous solution was attained. Hollow fibers were made by the solution spinning technique. The bore fluid was extruded through the spinneret using ISCO syringe pump. In the next step, dope solution was pumped to the spinneret under the N_2 atmosphere. Hollow fibers were kept in water for at least 24 hours and then in aqueous ethanol solutions with ethanol for 15min. The jet–stretch (JS) ratios of the spin line were manipulated by adjusting the take-up rate. The JS ratio is defined as the following equations.

$$JS = \frac{V_2}{V_1} \tag{1}$$

V_1 is the linear extrusion rate of the extruded fiber (cm/s), while V_2 is the rate at which the fiber is collected at the end of the spin line i.e. take-up rate (cm/s). Fig. 1 shows the schematic of experimental setup. Spinning parameters are listed in Table 1.

Membrane characterization

The thermal stability of polyurethane MMMs was studied by thermogravimetric analysis (TGA) within the temperature range of 25–850 °C at 10 °C·min^{-1}. The morphology of MMMs was investigated using a FE-SEM, Hitachi S-900. Differential scanning calorimetry (DSC) analysis was performed using a PerkinElmer DSC 8000 calorimeter.

Gas Separation Performance

The constant-volume apparatus (Aramis CS1325, Iran) was used to test the membranes permeabilities. The membrane module was sealed with gasket in a stainless steel cell

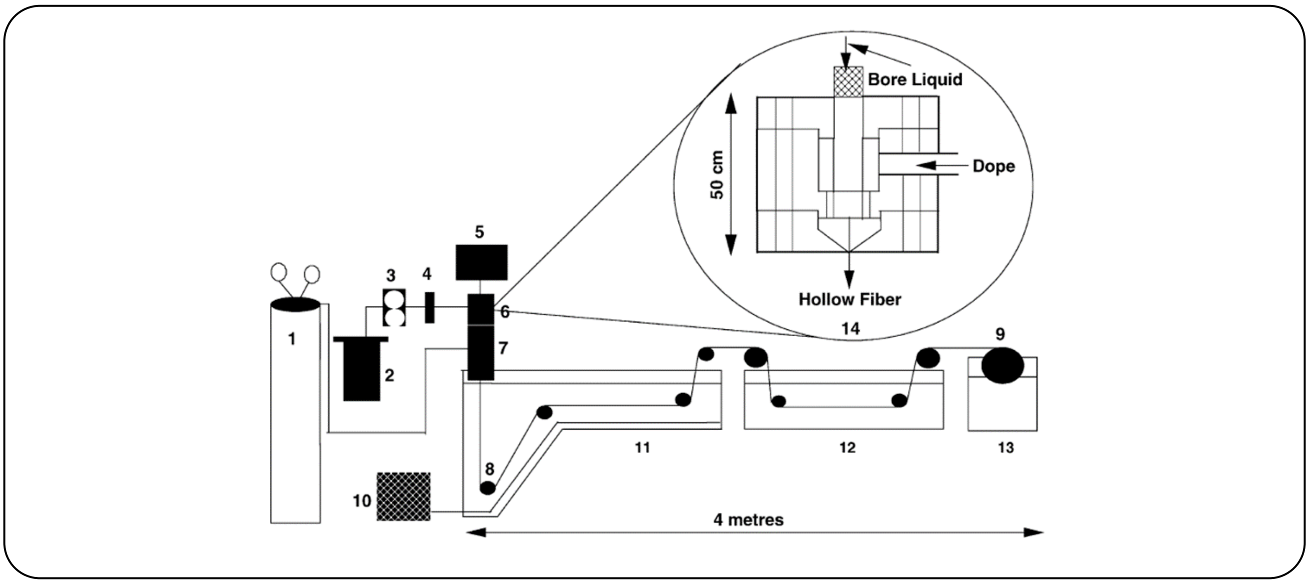

Fig. 1: Hollow fiber membrane spinning system: (1) nitrogen cylinder; (2) dope reservoir; (3) gear pump; (4) on-line filter, 7 mm; (5) syringe pump; (6) spinneret; (7) forced convective tube; (8) roller; (9) wind-up drum; (10) refrigeration/heating unit; (11) coagulation bath; (12) washing/treatment bath; (13) wind-up bath; and (14) schematic spinneret.

which was fixed inside an oven. The feed pressure of gases in feed stream was controlled by pressure sensors (2.600 G BD pressure sensors, accuracy of 0.25 FSO and DMP 343 BD pressure sensor, accuracy of 0.175% FSO, 1 mbar) and flow rates of gases were controlled using mass flow controllers (MKS Instruments). Temperature sensor (PT-100 sensors, accuracy of 0.1 K) was used. CO_2 and CH_4 permeation of the membranes were measured at feed flow rates of the gases 200 ml/min. The pressure-normalized flux or permeance, (P_i/l) was calculated by the equation:

$$\frac{P_i}{l} = \frac{N}{\Delta P} = \frac{Q}{A \times \Delta P}\left(\frac{273.15 \times 10^6}{T}\right) \quad (2)$$

$$\alpha_{ij} = \frac{\frac{P_i}{l_i}}{\frac{P_j}{l_j}} \quad (3)$$

where (P_i/l) is the gas permeance of a membrane in GPU (1 GPU = 1 × 10^{-6} cm^3(STP)/cm^2 s cmHg), *I* represents the penetrating gas *i*, Q_i is the volumetric flow rate of gas permeated through the membrane (cm^3/s, STP), *A* the effective membrane area (cm^2), ΔP is the trans-membrane pressure (cmHg), and *T* is the temperature at which the permeation experiment being performed. Chromatograph (Perkin Elmer) was used to investigate the the composition of gases side. α_{ij} represents ideal selectivity of gas *i* to *j*.

Experimental design

To extract mathematical model, find the most impact factor, the response surface methodology was used. If all variables are assumed measurable, the response surface can be expressed as follows:

$$y = f(x_1, x_2, \ldots, x_k) \quad (3)$$

Second order polynomial is usually considered as a full model in RSM[12-13]:

$$y = \beta_0 + \sum_{i=1}^{k} \beta_i x_i + \sum_{i=1}^{k} \beta_{ii} x_{ii}^2 + \sum_{i=1}^{k} \beta_{ij} x_i x_j + \varepsilon \quad (4)$$

where *y* is the response (CO_2 permeation), βs are regression coefficients, x_i is a coded independent variable, ε is the error and *k* is the number of factors. After optimizing membrane performance, the effect of stretch ratio(A), Zeolite content(B) and air gap distance (C) on membrane CO_2 and CH_4 permeability and selectivity was investigated at optimized condition.

Simulation and optimization of process configurations

The simulation method adapted in current work was conducted in Aspen Hysis. The hollow fiber membrane

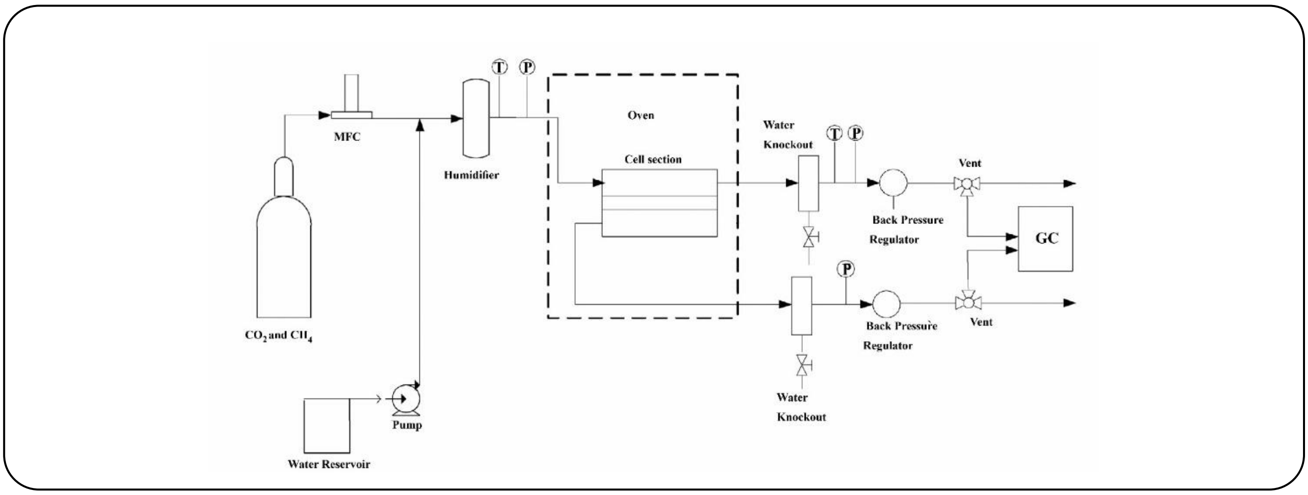

Fig. 2: Schematic diagram of the experimental set-up.

unit operation extension is comprised of two independent constituents, namely the ActiveX Server dynamic link library (DLL) and extension definition file (EDF). The adopted algorithm is robust, efficient, and converges at the stage cuts as high as 99.0%. The convergence was determined by an error function with a default composition calculation tolerance of 0.001%. The overall workflow was presented in Fig. 3.

The input parameters used for the simulation condition are summarized in Table 1. The gas processing cost (GPC) is calculated according to the procedure and fundamental assumptions outlined in Table 2 and the data obtained from process simulation. The proposed design configurations include single stage (SS), single stage with permeate recycle (SSPR), double stage with permeate recycle (DDPR), double stage with retentate recycle (DSRR), triple stage with retentate recycle (TSRR) and triple stage with permeate and retentate recycle (TSPRR).

RESULTSA AND DISCUSSION

Membrane characterization

To find the most suitable spinning conditions for SAPO-34/PES mixed matrix dope, the effects of air gap distance was first studied since this parameter can be easily manipulated throughout the process. SAPO-34/PES hollow fiber air gap distance varied from 10 to 25 cm. Fig. 5 shows the FESEM images of cross-sectional view of MMMs with different air gap distance. Referring to Fig. 5, macro-voids are produced in resultant SAPO-34/PES at the air gap distance of 5 cm and 10 cm. Table 3 records the gas permeation data for SAPO-34/PES hollow

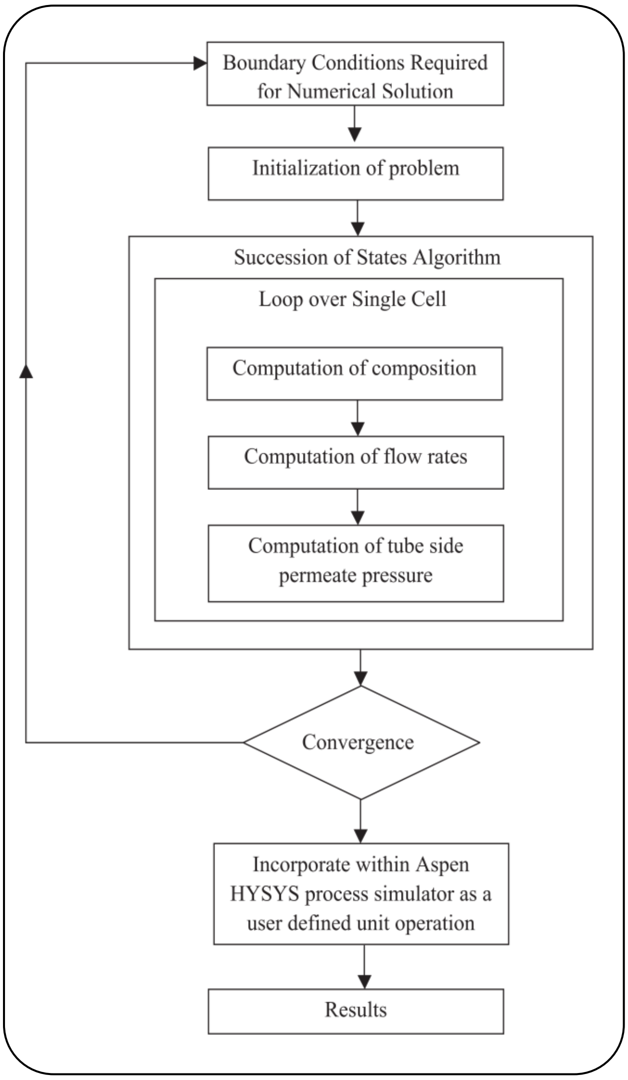

Fig. 3: Overall solution procedure for the hollow fiber membrane module simulation[14].

Table 1: Input parameters used for the simulation condition.

Membrane module specification	0.2032 m diameter (1 m × 18.5 m × 0.008 m channels)
Feed flow	35 MMSCFD (991,095 std.m^3/day)
Feed inlet pressure and temperature (typical offshore natural gas)	30 bar and 25 °C
Feed Composition(mole %)	10-60 CO_2 , balance CH_4, 0.05 C_2H_6,, 0.05 C_3H_8 ,0.1 N_2
Permeate pressure (bar)	1.4
CH_4 permeance	4.5E−06 cm^3 (STP) cm^{-2} s^{-1} $cmHg^{-1}$
CO_2/CH_4 selectivity	20
Residue CO_2 composition	<2% to meet pipeline specification
Membrane Fiber characteristic(inner/outer diameter)	250/100
Membrane Porosity	0.5
Effective membrane thickness	1000 Å (3.937 × 10^{-3} mil)
Membrane module diameter	15 in

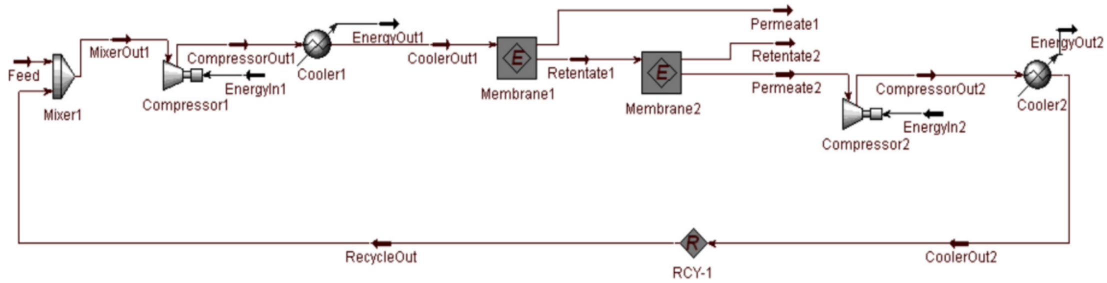

***Fig. 4: Basic simulated model*.**

fibers spun. Referring to Table, CO_2 and CH_4 permeances were decreased while gas pair selectivities were increased on the increment of air-gap distance from 5 cm to 15 cm. The reduction in gases permeance could be because of reduction of non-selective voids from the selective layer of MMMs[15].

RSM results

The analysis of variance (ANOVA) for removal efficiency (Y) is represented in Table 4. The correlation coefficient (R^2) is 0.99, which it is greater than 0.80, the cut-off for a model with good fit. The final regression model is presented in terms of its coded factors:

$$Y = 6.190 + 0.3314 \times A + 0.1577 \times B + 0.2728 \times C + 0.1669 \times AB + 0.1846 \times AC + 0.0511 \times BC - 0.1045 \times A^2 - 0.6540 \times B^2 - 0.4977 \times C^2$$

Where: stretch ratio(A), Zeolite content(B) and air gap distance (C).

Figs.6 shows the interaction effect of factors on response parameter. Based on the Figure, SR has a positive effect on CO2 permeability. Increasing SR results in decreasing membrane thickness which leads to improving mass transfer rate. Permeance and selectivity of stretched fibers were exceptionally better relative to non-stretched fiber. Based on the Fig.6b SAPO-34 presence has a synergetic effect on CO2 permeability. SAPO-34 zeolite is one of the inorganic materials that has been extensively employed in the synthesis of MMM for CO_2 gas separation. The molecular structure of SAPO-34 with pore size around 0.38 nm makes it as a promising filler for CO_2/CH_4 gas separation application since it is larger than CO_2 gas kinetic diameter (0.33 nm) and similar with CH_4 kinetic diameter (0. 38 nm). Fig.6c shows the effect of air

Table 2: Gas processing cost (GPC).

Total plant investment (TPI):	TPI=TFI+SC
Membrane module cost (MC)	$10/ft^2 (includes cost of membrane element)
Installed compressor cost (CC)	$8650 × (HP/η)$^{0.82}$ (for processes with recycle streams)
Fixed cost (FC)	MC+CC
Base plant cost (BPC)	1.12 * FC
Project contingency (PC)	0.20 * BPC
Total facilities investment (TFI)	BPC+PC
Start up cost (SC)	0.10 * VOM
Annual variable operating and maintenance Cost(VOM):	VOM=CMC+LTI+DL+LOC+MRC+UC
Contract and material maintenance cost(CMC)	0.05 * TFI
Local taxes and insurance (LTI)	0.015 * TFI
Direct Labor cost (DL) (based on 8 h/day per 25 MMSCFD of feed)	$ 15/h
Labor overhead cost (LOC)	1.15 * DL
Membrane replacement costs (MRC)	$ 3/ft^2 of membrane
Utility cost (UC)	$ 0.07/kw h
Wellhead price of crude natural gas	$ 2/MMBTU
Heating value of natural gas	1066.8 MMBTU/MMSCF
On stream factor (OSF)	96%
Compressor efficiency (η_{cp})	0.8

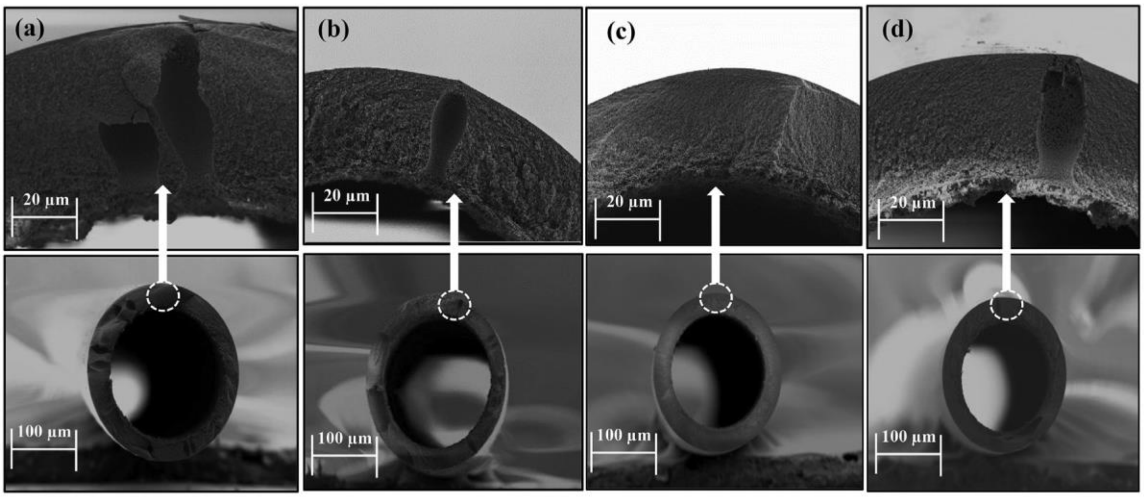

Fig. 5: FESEM images of cross-sectional view of SAPO-34/PES with different air gap distance of; (a) 5 cm, (b) 10 cm, (c) 15.0 cm, (d)20 cm.

Table 3: Effect of various air gap distance on hollow fiber permeation properties.

Air gap Distance(cm)	Permeance, GPU[a]		Selectivity
	CH_4	CO_2	CO_2/CH_4
5	5.60 ± 0.16	95.30 ± 13.08	17.02
10	4.11 ± 0.12	86.42 ± 10.06	21.02
15	2.87 ± 0.08	73.15 ± 1.08	25.48
20	3.32 ± 0.23	75.90 ± 3.85	22.86

[a] *1 GPU = 1 × 10^{-6} cm^3 (STP)/cm^2 s cmHg.*

Table 4: ANOVA results.

Source	Sum of Squares	DF	Mean Square	F-value	p-value	
Model	12.26	9	1.36	44.88	< 0.0001	significant
A	1.50	1	1.50	49.41	< 0.0001	
B	0.3397	1	0.3397	11.19	0.0074	
C	1.02	1	1.02	33.48	0.0002	
AB	0.2228	1	0.2228	7.34	0.0220	
AC	0.2727	1	0.2727	8.98	0.0134	
BC	0.0209	1	0.0209	0.6889	0.4259	
A^2	0.1575	1	0.1575	5.19	0.0459	
B^2	6.16	1	6.16	203.04	< 0.0001	
C^2	3.57	1	3.57	117.60	< 0.0001	
Residual	0.3036	10	0.0304			
Lack of Fit	0.2490	5	0.0498	4.56	0.0607	not significant
Pure Error	0.0546	5	0.0109			
Cor Total	12.56	19				

gap distance on CO_2 permeability. In low air gap distance, radial flow of solvent is not fully established and it cannot hinder the diffusion of external coagulant. Therefore finger-like macro-voids on cross-section of SAPO-34/PES are eliminated. This results leads to decrease CO2 permeability inside the membrane.

Maximum permeability and the corresponding optimal conditions of variables were determined and the model was confirmed by some further experimental runs. Numerical optimization was done to find a maximum point for the desirability function by setting the values of SR, SAPO-34 content and air gap distance within their ranges and maximizing the permeability. The results listed in Table 5. The desirability value was found to be 0.93. This optimum condition was checked experimentally. The results showed the permeability of 6.67×10^{-6} (cm^3(STP)/cm^2.cmHg.s). The high degree of agreement between the predicted optimum conditions and the repeated experimental results indicated that the CCD RSM could be employed as an effective and reliable tool for evaluation and optimization of the effects of parameters on the permeability.

CO_2/CH_4 separation experiments

Fig. 7 present CO_2 and CH_4 permeabilities of the PES/SAPO-34 MMMs as a function of upstream pressure. As observed, the both permeabilities decreases with increment of pressure.

Effect of operating temperature from 303 to 343 K on permeability and selectivity of the PES/SAPO-34 MMMs

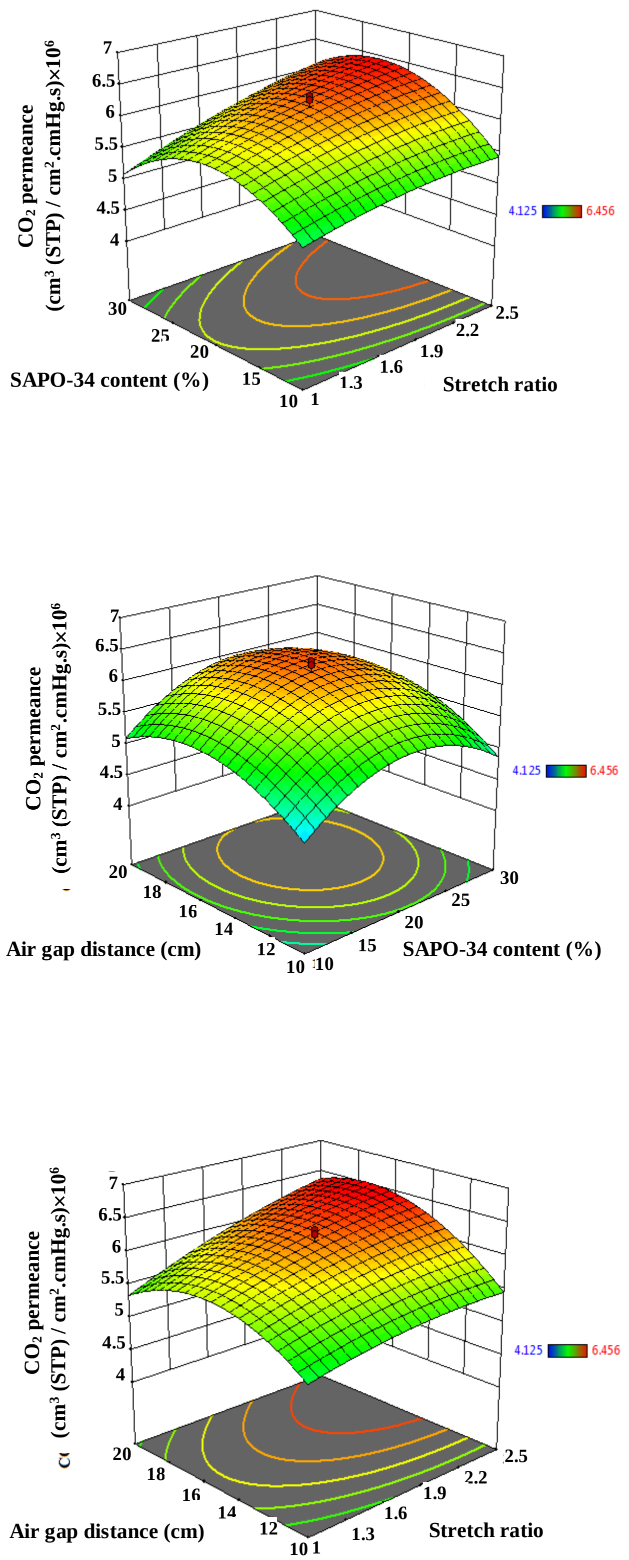

Fig. 6: 3D plot of factors effect on CO_2 permeability.

are presented in Fig. 8. As operating temperature is increases, permeabilities increase, while selectivity decreases. For CO_2 molecules, two different impacts are : solubility decreases with increasing temperature, while diffusivity increases with increasing temperature. Since the diffusivity is stronger function of temperature than solubility, permeability increases.

Comparison with other membranes

Table 6 has gathered the recently published CO_2/CH_4 separation performance of polysulfune-based MMM hollow fiber. Our developed SAPO34 MMM exhibited lower selectivity than that of other MMMs in the literature, but with a relatively high permeance.

Simulation Results

Fig. 9 shows the effect of feed composition on CH_4 recovery for all proposed configurations. It can be observed that the CH_4 recovery is reducing with the increase of CO_2 in the feed gas. The simulated results proved that the employing multiple stage systems leads to high methane recovery.

Fig. 10 shows the effect of feed composition on the total membrane area. It was found that the area rises with the CO_2 composition increment in the feed until it reaches its maximum point. Then, more increasing results in decreasing in the membrane area requirement.

To find the best design, GPC has to be minimum with respect to the operating conditions. Fig. 11 shows the effect of feed composition on the GPC. Single stage systems without recycle (SS) shows a moderate GPC since no compressors are needed and the area required is small. DSRR and triple TSPRR show the maximum GPC due to the high compressor power and very large membrane area required. TSRR results relatively less GPC because of the improved methane recovery.

CONCLUSIONS

In this work, the defects in polethersulfone (PES)/silicoaluminophosphate (SAPO)-34 zeolite mixed matrix membrane was prepared by dry–wet spinning technique for the separation of CO_2/CH_4 mixtures. In this regard, the synthesized PES/SAPO-34 mixed matrix membranes (MMMs) were characterized via FESEM analyses. It was found that air gap height gave the most influence on gas permeation properties. The effects of

Table 5: Optimised conditions

SR	2.5
SAPO-34 content	23.7%
Air gap distance	18
CO2 permeability	6.54×10^{-6} (cm^3(STP)/cm^2.cmHg.s)

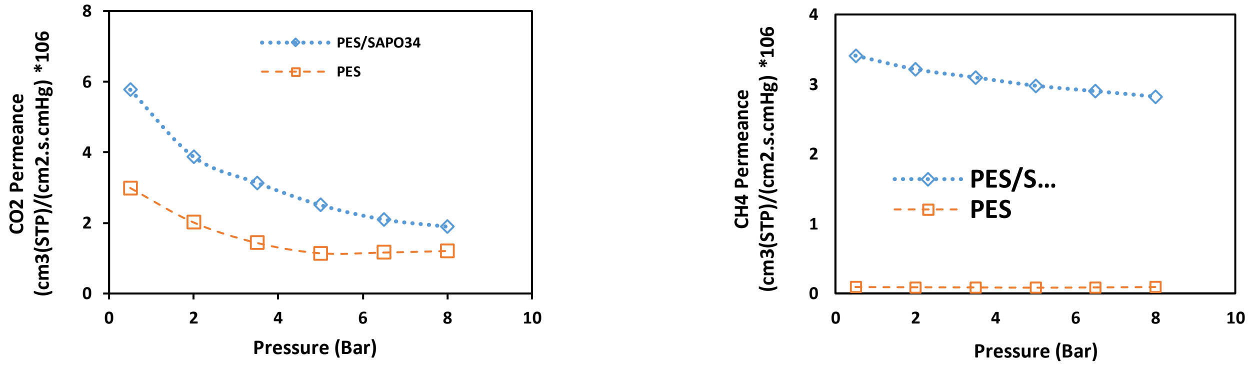

Fig. 7: Effect of feed pressure on a:CO2 b:CH4 permeance of the MMMs.

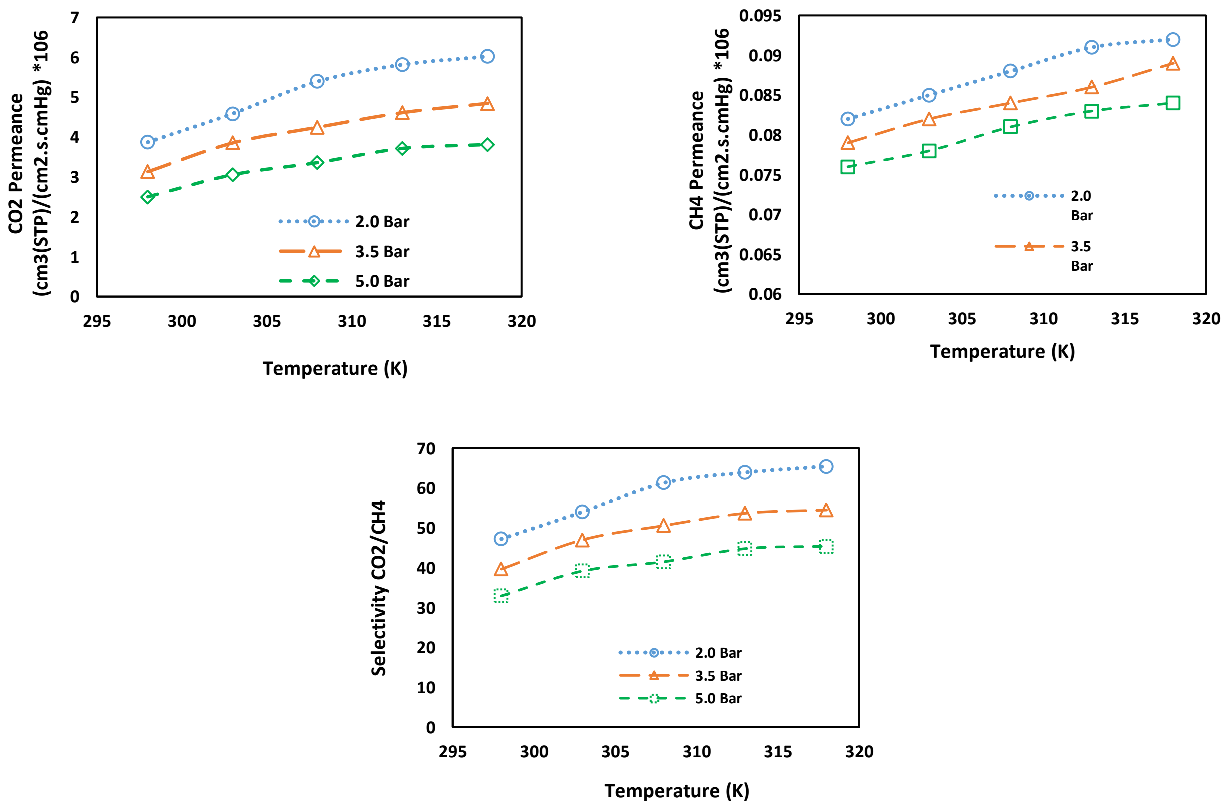

Fig. 8: Effect of feed temperature on a:CO2 b:CH4 permeance c: selectivity of the PES/SAPO-34.

Table 6: A comparison of PES/SAPO 34 hollow fiber mixed matrix membranes for CO_2/CH_4 separation.

Membrane	Permeance, GPU		Selectivity	Ref.
	CH4	CO2	CO2/CH4	
PSF	2.52	78.11	31.05	[26]
PSF + 0.1% fumed silica	2.75	90.04	32.74	[26]
PSF + 2% carbon black	2.16	76.25	35.40	[27]
PSF + 5% μCX	2.45	95.40	39.10	[28]
PSF	2.19	60.09	27.44	[16]
PSF + 0.05% Cloisite® 15A	1.41	56.25	40.26	[16]
ZIF-8/Pebax 1657/PES	52	542	16.1	[17]
NaY zeolite- Matrimid®5218 matrix			43.3	[18]
ABS/PVAc		40.41	4.93	[19]
Pebax 1657/ ZIF-8			20.4	[20]
NaX/PES		187.76	57.41	[21]
PES/SAPO-34	3.41	96.25	28.22	Present Study

μCX = microporous carbon xerogel.

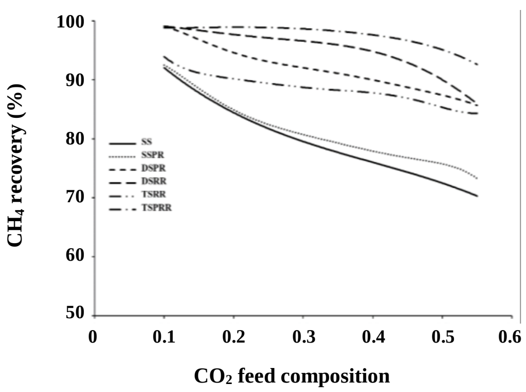

Fig. 9: Effect of feed composition on methane recovery.

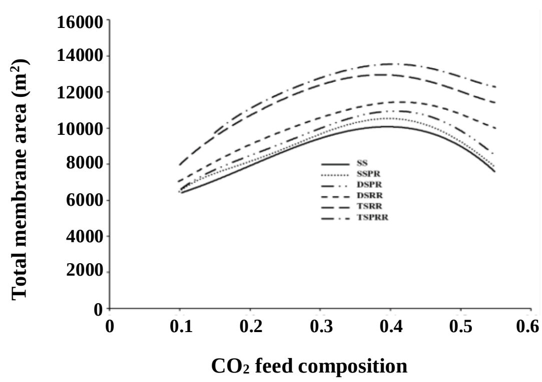

Fig. 10: Effect of feed composition on total membrane area.

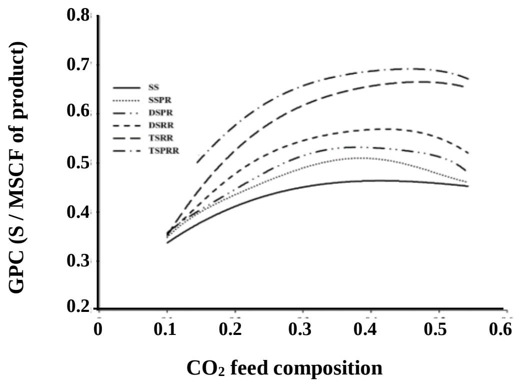

Fig. 11: Effect of feed composition on gas processing cost.

modified feed temperature and feed pressure on permeation and CO_2/CH_4 selectivity of membranes were investigated. The MMMs showed better performance than the neat PES membrane. The maximum selectivity achieved was 28.22 at 0.5 bar pressure and 35 °C. The minimum GPC is achieved by the double stage system with permeate recycle because of the high methane recovery and moderate power requirement for the configuration.

Received : Nov. 12, 2019 ; Accepted : Jan. 13, 2020

REFERENCES

[1] Rezakazemi M., Sadrzadeh M., Matsuura T., Thermally Stable Polymers for Advanced High-Performance Gas Separation Membranes, *Prog. Energy Combust. Sci.*, **66**: 1-41 (2018).

[2] Razavi S.M.R., Rezakazemi M., Albadarin A.B., and Shirazian S., Simulation of CO_2 Absorption by Solution of Ammonium Ionic Liquid in Hollow-Fiber Contactors, *Chem. Eng. Process.: Process Intensif.*, **108**: 27-34 (2016).

[3] Hosseinzadeh Helaleh A., Alizadeh M., Performance Prediction Model of Miscible Surfactant-CO_2 Displacement in Porous Media Using Support Vector Machine Regression with Parameters Selected by Ant Colony Optimization, *Journal of Natural Gas Science and Engineering*, **30**: 388-404 (2016).

[4] Soroush E., Shahsavari S., Mesbah M., Rezakazemi M., Zhang Z., A Robust Predictive Tool for Estimating CO_2 Solubility In Potassium Based Amino Acid Salt Solutions, *Chin J Chem Eng*, **26(4)**: 740-746 (2018).

[5] Rezakazemi M., Heydari I., Zhang Z., Hybrid Systems: Combining Membrane and Absorption Technologies Leads to More Efficient Acid Gases (CO_2 and H_2S) Removal from Natural Gas, *J. CO_2 Util.*, **18**: 362-369 (2017).

[6] Kambarani M., Bahmanyar H., Mousavian M.A., Mousavi S.M., Crossflow Filtration of Sodium Chloride Solution by A Polymeric Nano Flter: Minimization of Concentration Polarization by a Novel Backpulsing Method, *Iran. J. Chem. Chem. Eng. (IJCCE)*, **35(4)**: 135-141 (2016).

[7] Mandanipour V., Noroozifar M., Alam A.R.M.-., Khorasani-Motlagh M., Fabrication and Characterization of a Conductive Proton Exchange Membrane Based on Sulfonated Polystyrenedivinylbenzene Resin-Polyethylene (SPSDR-PE): Application in Direct Methanol Fuel Cells, *Iran. J. Chem. Chem. Eng. (IJCCE)*, **36(6)**: 151-162 (2017).

[8] Ahmad N.N.R., Mukhtar H., Mohshim D.F., Nasir R., Man Z., Effect of Different Organic Amino Cations on SAPO-34 for PES/SAPO-34 Mixed Matrix Membranes Toward CO_2/CH_4 Separation, *J. Appl. Polym. Sci.*, **133(18)**: - (2016).

[9] Rezakazemi M., Mohammadi T., Gas Sorption in H_2-Selective Mixed Matrix Membranes: Experimental and Neural Network Modeling. *International Journal of Hydrogen Energy*, **38(32)**: 14035-14041 (2013).

[10] Otitoju T.A., Saari R.A., Ahmad A.L., Progress in the Modification of Reverse Osmosis (RO) Membranes for Enhanced Performance, *J. Ind. Eng. Chem.*, **67**: 52-71 (2018).

[11] Li S., Alvarado G., Noble R.D., Falconer J.L., Effects of Impurities on CO_2/CH_4 Separations Through SAPO-34 Membranes, *J. Membr. Sci.*, **251(1-2)**: 59-66 (2005).

[12] Alizadeh M., Sadrameli S.M., Numerical Modeling and Optimization of Thermal Comfort in Building: Central Composite Design and CFD Simulation, *Energy and Buildings*, **164**: 187-202 (2018).

[13] Wahab M.F.A., Ismail A.F., Shilton S.J., Studies on Gas Permeation Performance of Asymmetric Polysulfone Hollow Fiber Mixed Matrix Membranes Using Nanosized Fumed Silica as Fillers, *Sep. Purif. Technol.*, **86**: 41-48 (2012).

[14] Safarvand D., Aliazdeh M., Giri M.S., Jafarnejad M., Exergy Analysis of NGL Recovery Plant Using a Hybrid ACOR-BP Neural Network Modeling: A Case Study, *Asia-Pacific Journal of Chemical Engineering*, **10(1)**: 133-153 (2015).

[15] Kim K., Ingole P.G., Kim J., Lee H., Separation Performance of PEBAX/PEI Hollow Fiber Composite Membrane for $SO_2/CO_2/N_2$ Mixed Gas, *Chem. Eng. J.*, **233**: 242-250 (2013).

16. Zulhairun A.K., Ng B.C., Ismail A.F., Surya Murali R., Abdullah M.S., Production of Mixed Matrix Hollow Fiber Membrane for CO_2/CH_4 Separation, *Sep. Purif. Technol.*, **137**: 1-12 (2014).

[17] Jomekian A., Behbahani R.M., Mohammadi T., Kargari A., CO_2/CH_4 Separation by High Performance co-Casted ZIF-8/Pebax 1657/PES Mixed Matrix Membrane, *J. Nat. Gas Sci. Eng.*, **31**: 562-574 (2016).

[18] Amooghin A.E., Omidkhah M., Kargari A., Enhanced CO_2 Transport Properties of Membranes by Embedding Nano-Porous Zeolite Particles Into Matrimid®5218 Matrix, *RSC Adv.*, **(5)**: 8552-8565 (2015).

[19] Sanaeepur H., Amooghin A.E., Moghadassi A., Kargari A., Preparation And Characterization of Acrylonitrile–Butadiene–Styrene/Poly (vinyl acetate) Membrane for CO_2 Removal, *Sep. Purif. Technol.*, **80(3)**: 499-508 (2011).

[20] Jomekian A., Bazooyar B., Behbahani R.M., Mohammadi T., and Kargari A., Ionic Liquid-Modified Pebax® 1657 Membrane Filled by ZIF-8 Particles for Separation of CO_2 from CH_4, N_2 and H_2, *J. Membr. Sci.*, **524(1)**: 652–662 (2017).

[21] Maleha M.S., Raisi A., CO2-Philic Moderate Selective Layer Mixed Matrix Membranes Containing Surface Functionalized NaX Towards Highly-Efficient CO_2 Capture, *RSC Adv.*, **9**: 15542 - 15553 (2019).